Isolating Orographic Effects on Hurricane Ivan (2004) through Numerical Modeling

Steven Harville

North Carolina State University: Marine, Earth and Atmospheric Sciences

1 Introduction

There is much to be learned about Atlantic hurricanes, and much incentive to learn. The strong winds, flooding rain, high waves, and damaging storm surge which accompany a typical season of landfalling hurricanes can cause billions in damage. Ivan, a 2004 hurricane reaching category-5 strength on three separate occasions, was no exception, causing an estimated $14 billion (Franklin et al. 2006). It was one of the strongest tropical cyclones on record with maximum sustained winds of 145kt and a minimum pressure of 910hPa. It made landfall as a Saffir-Simpson category-3 storm (105kt winds) along the small section of land comprising Alabama's southern shoreline at approximately 0650 UTC September 16. This experiment focuses on the orographic lifting mechanism of the Appalachian mountain chain in forcing hurricane winds upwards, leading to heavy precipitation. Figure 1 shows the path and category of Ivan as it moved from the Atlantic basin, eventually weakening to tropical depression strength as it impinged upon the Appalachian mountains.

2 Ivan Synopsis

The initial disturbance eventually to become Ivan was a tropical wave that left the west coast of Africa on August 31st (Franklin et al. 2006). As convection increased, a tropical

depression formed around 1800 UTC, 2 September. It realized tropical storm strength the next day, and continued to strengthen, becoming a category-1 hurricane by 0600 UTC, 5 September. Over the next 18 hours, its minimum central pressure fell 40hPa, and winds of 115kt were observed within the category-4 storm.

After a brief stint of weakening, Ivan regained category-3 strength before its northern eyewall passed directly over Granada at 2130 UTC, 7 September. From there, Ivan continued to strengthen, making category-5 strength some 32 hours later just south of the Dominican Republic. As the storm slowly moved westward, Jamaica narrowly avoided a direct strike with a last minute shift in storm track on September 11^{th}. The island also benefited from a well-timed eyewall replacement cycle. Ivan reached its maximum intensity hours later at 0000 UTC, 12 September with 145kt winds and a central pressure low of 910hPa.

The next day, after weakening yet again, the dangerous storm regained category-5 strength as it passed over warm Caribbean waters (Franklin et al. 2006). Meanwhile, upper air divergence from an approaching mid-latitude trough enhanced Ivan's outflow region, and the storm held category-5 intensity over the next 30 hours. Gradual weakening ensued as the storm was influenced by another mid-latitude system and the vertical shear associated with it. Prior to landfall, the shear intensified and became more westerly, bringing drier air into the core of the storm. Despite this, Ivan maintained category-3 strength as it made landfall to the west of Gulf Shores, Alabama at 0650 UTC, 16 September.

As the storm made landfall, a weak trough was centered northwest of Ivan's position while a subtropical high was set up to the east (Fig. 2a). The two pressure anomalies remained nearly stationary relative to the tropical cyclone through the study period (Fig. 2a-d), each contributing to a general steering flow towards the northeast. A look at PV cross-sections across the two anomalies (not shown) gives no indication of mutual amplification through time .

Accumulated rainfall (shown later) was summed for the duration of the study period starting 0600 UTC, 16 September and ending 0000 UTC, 18 September as Ivan began transitioning into an extratropical storm (Franklin et al. 2006). Heaviest precipitation during the passage of Ivan occurred along eastern (windward) slopes. Franklin et al. (2006) reports precipitation totals in various locations. Rainfall greater than 200mm fell in large swaths across Alabama, western Florida, and the eastern Tennessee valley. Highest rainfall totals from the NARR were calculated at 159mm. The highest rainfall point measurements fell over Pensacola (401mm) and Cruso, NC (432mm). Widespread flooding resulted as many areas were still wet from Hurricane Frances and Tropical Storm Bonnie.

Its worth briefly mentioning just how powerful this storm was as evidenced by some of the records it set. It was the southernmost cyclone to gain major hurricane strength on record. The longest in recent records (since 1944, the year reconnaissance began), it spent a total of 10 non-consecutive days as a major hurricane, and eight consecutive days as a category-4 storm or higher. It came close to breaking the lowest minimum pressure observed. As of 2004, its minimum pressure of 910hPa was broken by only five storms before it.

3 Data and Methodology

This study employs the Weather Research and Forecasting Model (WRF) to simulate Hurricane Ivan. Two simulations were run: 1) TOPO whose goal it was to replicate observations of the actual storm, and 2) UNTOPO, the same as the first run with the topography removed. The strategy here is simple. The use of modeling allows for the quantification of differences in precipitation and other related variables. By comparing the two runs using a strictly mathematical framework, we can both isolate and quantify the effects of the mountains on hurricane precipitation structure and intensity. Numerical simulations were initialized far from the area of interest in an effort to reduce any unwanted effects of removing

terrain, and to ensure sufficient time for the atmosphere to adjust. The modeled forecast period starts 0000 UTC September 12, 2004 and ends one week later (0000 UTC September 19). Because storm propagation speeds differed between the two runs, and to the observed track, comparisons were realized by spatially anchoring the storm at key locations. Events were defined starting at landfall, and ending upon crossing the North Carolina-Virginia border.

Data for model initial conditions were supplied by the National Centers for Environmental Prediction (NCEP) High Resolution Global Forecast System (1 degree GFS). Results from the TOPO model run were compared against the North American Regional Reanalysis (NARR) dataset and the Atlantic basin hurricane database (HURDAT).

3.1 Weather Research and Forecasting Model

The WRF model comes principally from the collaborative efforts of the National Center for Atmospheric Research (NCAR) and NCEP. We use the Advanced Research WRF (ARW) version in this study. Each of the two runs were exactly similar with respect to domain, initial conditions, and physical schemes, the only difference being the removal of all topography in the UNTOPO run. Initial conditions (as well as six hourly updated boundary conditions) come from NCEP's high resolution GFS. The model was run on a Lambert conformal grid with a domain chosen small enough to optimize computational efficiency, but large enough to keep boundaries far from the study area (Fig. 3). In order to maintain numerical stability, the ratio of grid spacing (km) to time step (s) should not exceed 6:1 (Skamarock et al. 2005). For moving-nest grids, a staunch 3:1 ratio must be used (Gentry 2007). With the potential for future nesting in mind, the horizontal grid spacing of 12 kilometers gave way to a time step of 36 seconds. There were 31 vertical levels with data output every three hours. We used the WSM 6-class graupel microphysics scheme along with a Kain-Fritsch convective parameterization. We chose to use the non-hydrostatic option for the model runs.

3.2 North American Regional Reanalysis

In order to get a sense of how well the model simulated actual observations, TOPO run output was compared against the NARR. The North American Regional Reanalysis covers the period 1979 to present (2006), and bases the temporal domain of the study. This reanalysis dataset comes from a blending of previous Eta model forecasts with an observational network (Mesinger et al. 2006). It goes beyond its Betts-Miller-Janjić convective parameterization adjustment scheme by assimilating observed precipitation. Lin et al. (1999) details the specifics of the 3D variational Eta Data Assimilation System (EDAS). This system is used for the creation (and improvement) of the NARR precipitation fields. Once precipitation occurs in the model, it is quantitatively compared to observations (WSR-88D radar and automated rain guages). Latent heating, water vapor mixing ratio, relative humidity, and cloud water mixing ratio values are correspondingly adjusted. In terms of reanalysis datasets, the NARR has superior resolution. It offers 32 kilometer grid spacing with 29 pressure levels, and reports at three hour intervals.

Although the NARR has the best spatial and temporal resolution for the study domain, of particular concern to this study are the findings of Grumm and Holmes (2007). It is their observation that the resolution of the NARR is still too coarse to find areas subject to flash flooding. Comparisons of the NARR with regional precipitation data show that while NARR fields maintain the overall precipitation pattern, it underestimates it by a factor of two or more. That being said, one should not rely on the NARR to quantify specific storm accumulations, but should instead use the data to identify coarse patterns of large-scale precipitation (Grumm and Holmes 2007). Identification of smaller-scale areas with the greatest potential for flash flooding will be the task of numerical simulations.

4 Results

First, a comparison is made between the TOPO simulation and the NARR data (as well as the HURDAT defined track) in order to ascertain how consistent model results are to observations. Afterwards, topographic effects will be isolated as we contrast the UNTOPO model output against the TOPO run.

4.1 TOPO vs. NARR/Observed

Because the model was initialized far from the study domain, there are inconsistencies between model runs and observations with regard to the timing of events. To regain consistency, we define study periods that draw basis on storm location, rather than specific times. Events begin at landfall and end as Ivan tracks across the North Carolina - Virginia border. Thus the observational study period as defined by the NARR begins at 0600 UTC, 16 September and ends at 0000 UTC, 18 September lasting 42 hours. The TOPO run begins at forecast hour 96 (0000 UTC 16, September), remaining in the study area for 45 hours until 2100 UTC, 17 September. Time for all datasets begins at zero as the storm makes landfall.

4.1.1 Track and Intensity

In order to show storm motion, and also to provide a visual sense of intensity, we take advantage of the observation that the pressure marking the center of a hurricane is typically the lowest within a finite domain. Upon finding the minimum domain-wide sea-level pressure, a new field was created at three-hour intervals for the NARR (Fig. 4, the TOPO control run (Fig. 5) and later, for the experimental UNTOPO simulation (Fig. 6). Minimum sea-level pressure (marking the hurricane center) is subtracted from mean sea-level pressure, leaving a field of positive pressure anomalies. The grid cell with a value of zero marks the storm center. Low pressure centers are defined by darkly filled shading, the outside of which marks the 0.25hPa perturbation above minimum. Beyond these shaded lows lie rings that increment

higher pressure anomalies outwards. The inner ring sits 1hPa outside the cyclone center, the next ring outward 2hPa, then 3hPa. The outermost ring contours the 5hPa positive pressure perturbation. In effect, the more compact these contours, the sharper the gradient between the storm center and surrounding environment, the more defined the hurricane low, and thus, the more intense the storm.

Hurricane Ivan six-hourly HURDAT-defined track positions are shown as reference alongside each of the resulting storm paths. Although the TOPO run (Fig. 5) shows small errors in track, the model adequately maintains correct course, with results similar to the NARR (Fig. 4). Both the control (Figs. 7c, 8c, 9c, 10c) and experimental simulations (with the Appalachians removed - Figs. 7e, 8e, 9e, 10e) track closely to observation, suggesting that non-linear interaction between Ivan and its synoptic environment was limited. With consideration to storm speed, however, the TOPO simulated storm outruns the observed. TOPO estimates landfall of Ivan at model hour 96 (0000 UTC September 16); almost seven hours to early.

As Ivan makes landfall in the TOPO run, intensity is at a maximum (Fig. 7c). In reality, Ivan was said to have slightly weakened over the gulf before making landfall as vertical shear increased from a moderate southwesterly flow ahead of an upper level trough over the central US (Franklin et al. 2006). After landfall, both datasets show general weakening (Figs. 8a and 8c), then similar flow evolution as Ivan comes into contact with the mountains and begins to break up (Figs. 9a and 9c).

4.1.2 Synoptic Pattern and Moisture Profiles

At landfall, the overall synoptic picture looks quite similar (Figs. 7a and 7c) with the TOPO run slightly shifted eastward. The upper-level jet to the north of the storm is slightly stronger in the TOPO simulation, attributable perhaps to the higher resolution of the WRF. By event's end, the NARR synoptic pattern (Fig. 10a) shows a stronger jet to the south of

the storm, with a more intensely developed downstream ridge.

Cross-sections of moisture and winds taken along fixed transects (shown with each respective synoptic map) at landfall (Fig. 7b and 7d) portray similar levels of moisture, especially at low levels. A plume of moist tropical air comes into the domain from the right (advected by southeasterly hurricane flow). Aloft, the NARR shows more sensitivity to the presence of topography than the TOPO run, despite having the lower resolution. A mountain-induced current is evidenced on the lee-side flow by a wave-like pattern of moisture layers and winds. Moisture patterns after landfall are consistent between observation and model run (Figs. 8b through 10b and 8d through 10d), despite the presence of stronger flow in the NARR.

4.1.3 ω Fields and Precipitation Structure

Vertical motion (Fig. 11a and 11c), plotted at times occurring after Ivan impinges upon the Appalachians (synchronous with figure 9) shows some similarity between the NARR and TOPO run. Much of the disparity may stem from numerical "noise" generated by the higher resolution WRF. Orographic lifting along southeastern, windward slopes is prominent in either dataset. Consistency is also retained between the two with regard to the strong vertical motion to the northwest, both resulting from strong upper-air divergence (Fig. 9a and 9c). Though more pronounced in the WRF, three-hour accumulated precipitation totals (Fig. 11b and 11d) show much similarity, and reflect patterns seen in ω fields with stronger signatures on windward slopes.

Total precipitation plots during defined event periods for the NARR (Fig. 12), TOPO (Fig. 13), and UNTOPO (Fig. 14) runs are included at the end for reference. The general patterns between TOPO and observed show marked similarity across terrain, though fields are typically more pronounced in the simulation. To the northeast, beyond the region of greatest mountain slope, the NARR shows more precipitation, and a more active outflow region than was simulated. The latent heating generated was responsible for intensifying the

downstream ridge (Fig. 10a).

4.2 TOPO vs. UNTOPO model runs

It was shown in the last section that the TOPO run verified with observations fairly well. Here, we repeat the same procedure between the two model runs in the hopes of finding a quantifiable orographic effect. The event period (45 hours) for the TOPO remains defined starting from forecast hour 96 (0000 UTC 16, September), ending at hour 141 (2100 UTC, 17 September). The faster propagation speed found in the UNTOPO simulation anchored its study period (39 hours) between forecast hours 90 (1800 UTC, 15 September) and 129 (0900 UTC, 17 September).

4.2.1 Track and Intensity

Given HURDAT track locations (red hurricane symbols) as spacial reference, the most immediate difference observed from the TOPO run (Fig. 5) is the eastward track deviation occurring in the UNTOPO (Fig. 6) experiment. The storm also travels too fast, making landfall approximately six hours sooner than the TOPO run (nearly 13 hours earlier than observations). As was earlier noted with the TOPO simulation, UNTOPO similarly shows a tighter bullseye just prior to landfall, retaining some consistency in intensity from one run to the next. As expected, while the TOPO run begins to breakup on approach of the Appalachians, the UNTOPO run weakens in similar magnitude, but retains axisymmetric organization. Towards the end of the simulation, Hurricane Jeanne emerges to the southeast.

4.2.2 Synoptic Pattern and Moisture Profiles

Although plotted tracks show marked difference, the synoptic patterns, and their evolution through time look nearly identical between TOPO and UNTOPO runs (Figs. 7c through 10c and 7e through 10e). Cross-terrain moisture profiles also show similar structure, though higher concentrations of moisture are transported across the UNTOPO domain. While winds

are similar in horizontal magnitude, the vertical component is much weaker in all UNTOPO cross-sections with the exception of figure 9f.

4.2.3 ω Fields and Precipitation Structure

Signatures of ω (Fig. 11c and 11e) corresponding to this time period (Fig. 9) are consistent between model runs in areas well away from topography, while the TOPO simulation shows much more fragmentation along the range. These areas of vertical motion result in nearly identical precipitation signatures, with obvious exception in areas of high terrain.

Precipitation through each model run was totaled, with a difference field (TOPO-UNTOPO) calculated and shown by figure 15. Positive linear areas to the northwest (and negative to the southeast) portray the expected result that tracks between the two runs do not completely conform to one another. Over the topographic area of interest, the plot shows intuitive results, with the existence of local positive maxima on the windward side of the mountain. These maxima define orographically enhanced, problem-forecast areas that are particularly sensitive to heavy precipitation and potential flooding. Within these areas lie eight of the ten locations in Georgia, Tennessee, and North Carolina with observations reporting greater than 225mm of total accumulation.

5 Conclusions and Future Work

Using WRF-ARW, two numerical simulations are performed for hurricane Ivan (2004). The first (TOPO) seeks verification with the observed field (NARR). The second (UNTOPO) removes all topography from the domain, and proceeds using the same conditions as the first holding all else constant. The goal of the study to isolate and quantify orographic effects on impinging hurricanes to better understand the resulting increase in precipitation.

The TOPO run (versus the observed) shows excellent verification of the precipitation structure and intensity, as well as the path taken by the hurricane. The modeled storm

moves too quickly, however, making landfall nearly seven hours too early. In order to isolate and quantify orographic effect on hurricane precipitation, the TOPO run is compared to UNTOPO. Although the UNTOPO run shows deflection of the storm too far to the east, and propagating too quickly (making landfall nearly 13 hours before observation), conclusions may be drawn between the two runs, namely, from the precipitation analysis. The differencing of storm totals (TOPO-UNTOPO) show local maxima along windward slopes (Fig. 15). The TOPO total maximum value for this feature of 333mm, when compared to the same for the UNTOPO, amounts to a total precipitation difference of 223mm. This number may be somewhat misleading (and should not be used as an absolute quantifiable difference) owing to the definition of individual event periods. The TOPO simulation storm speed was slower than the UNTOPO after making landfall. As such, the TOPO 45-hour event had six hours longer to precipitate onto the study domain.

The scope of this study was Hurricane Ivan, representative of but one category out of four general track orientations. Future model runs will tackle hurricanes that approach the study domain at contrasting angles. With verification of the enhancement of precipitation by orographic forcing, an obvious first step nearing completion, the task at hand comes with the identification of small-scale features of highly variable, topographically sensitive precipitation hot spots. The next step is an analysis of local precipitation maxima, and the plotting of spatial distributions of the frequency of high threshold events with focus on the smallest-scale features resolvable by numerical simulations. It is hoped that forecasting for these problem areas will be much improved given a prior general knowledge of the orientation of the approach path.

References

Franklin, J. L., R. J. Pasch, L. A. Avila, J. L. Beven, M. B. Lawrence, S. R. Stewart, and

E. S. Blake, 2006: Atlantic Hurricane Season of 2004. *Mon. Wea. Rev.*, **134,** 981–1025.

Gentry, M S, 2007: Sensitivity of WRF Simulations of Hurricane Ivan to Horizontal Resolution. Master's thesis, North Carolina State University, Raleigh, North Carolina.

Grumm, R. H., and R. Holmes, 2007: Patterns of Heavy rainfall in the Mid-Atlantic Region. *22nd Conference on Weather Analysis and Forecasting/18th Conference on Numerical Weather Prediction*, page 5A.2.

Lin, Y., K. E. Mitchell, E. Rogers, M. E. Baldwin, and G. J. DiMego, 1999: Test assimilations of the realtime, multi-sensor hourly precipitation analysis into the NCEP Eta model. *Bull. Amer. Meteor. Soc.*, pages 341–344.

Mesinger, F., G. Dimego, E. Kalnay, K. Mitchell, P. C. Shafran, W. Ebisuzaki, D. Jovi, J. Woollen, E. Rogers, E. H. Berbery, M. B. Ek, Y. Fan, R. Grumbine, W. Higgins, H. Li, Y. Lin, G. Manikin, D. Parrish, and W. Shi, 2006: North American Regional Reanalysis. *Bulletin of the American Meteorological Society*, **87,** 343–360.

Skamarock, W. C., J. B. Klemp, J. Dudhia, D. O. Gill, D. M. Barker, W. Wang, and J. G. Powers, 2005: A description of the Advanced Research WRF Version 2. *Tech. Rep. NCAR/TN-468+STR.*

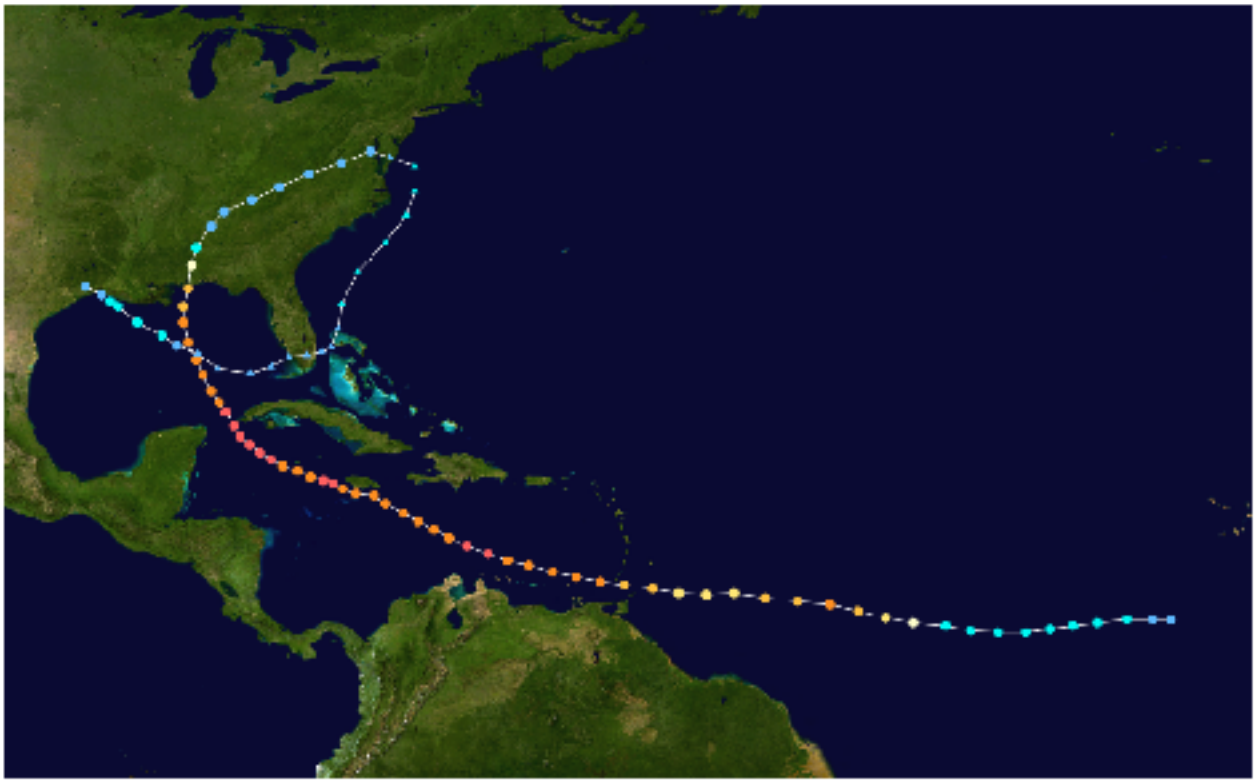

Figure 1: Observed track and category of Ivan

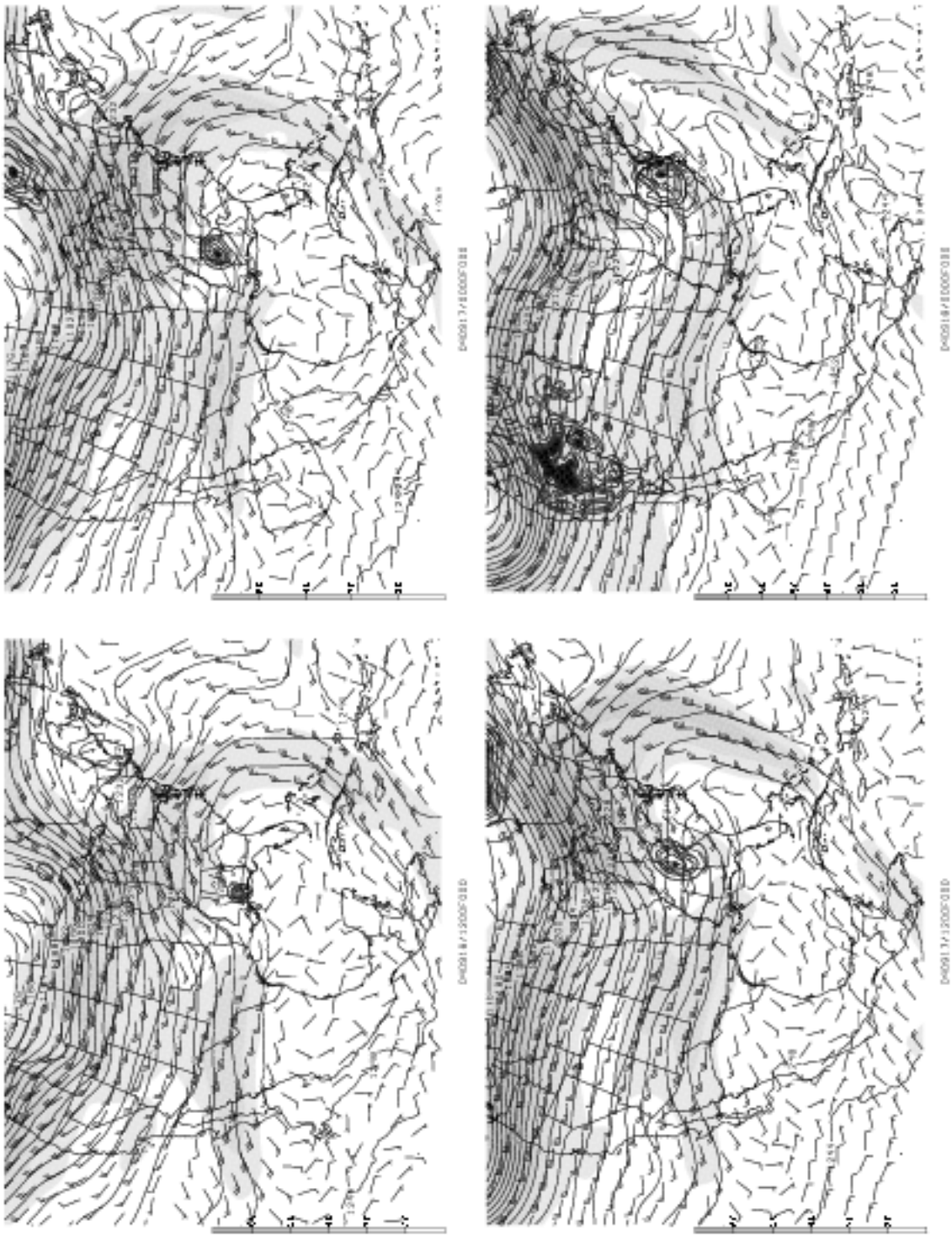

Figure 2: NARR 200hPa geopotential heights (dam) and winds (ms^{-1}) during Ivan: 9-16-04 1200UTC to 9-18-04 0000UTC

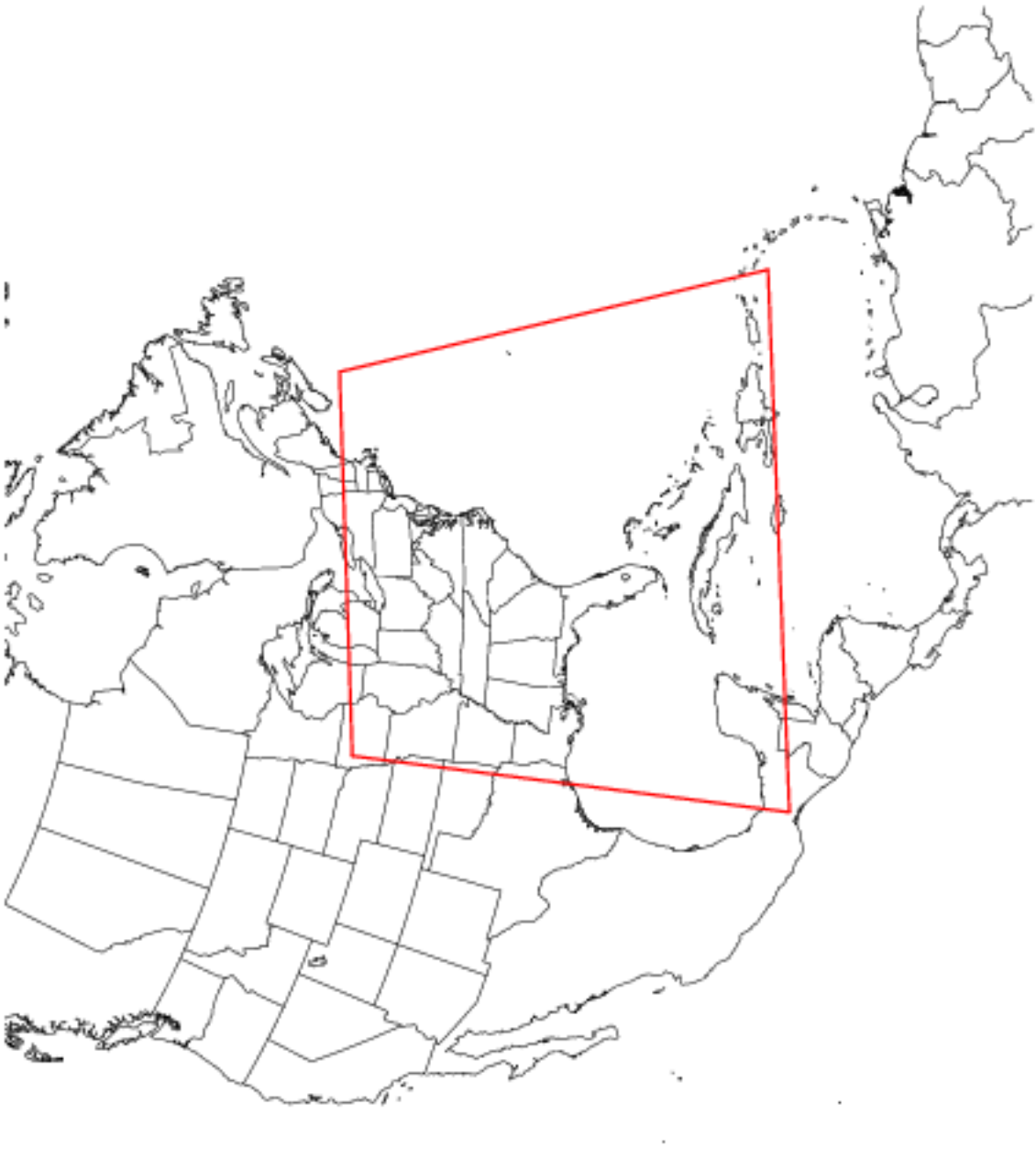

Figure 3: WRF model domain

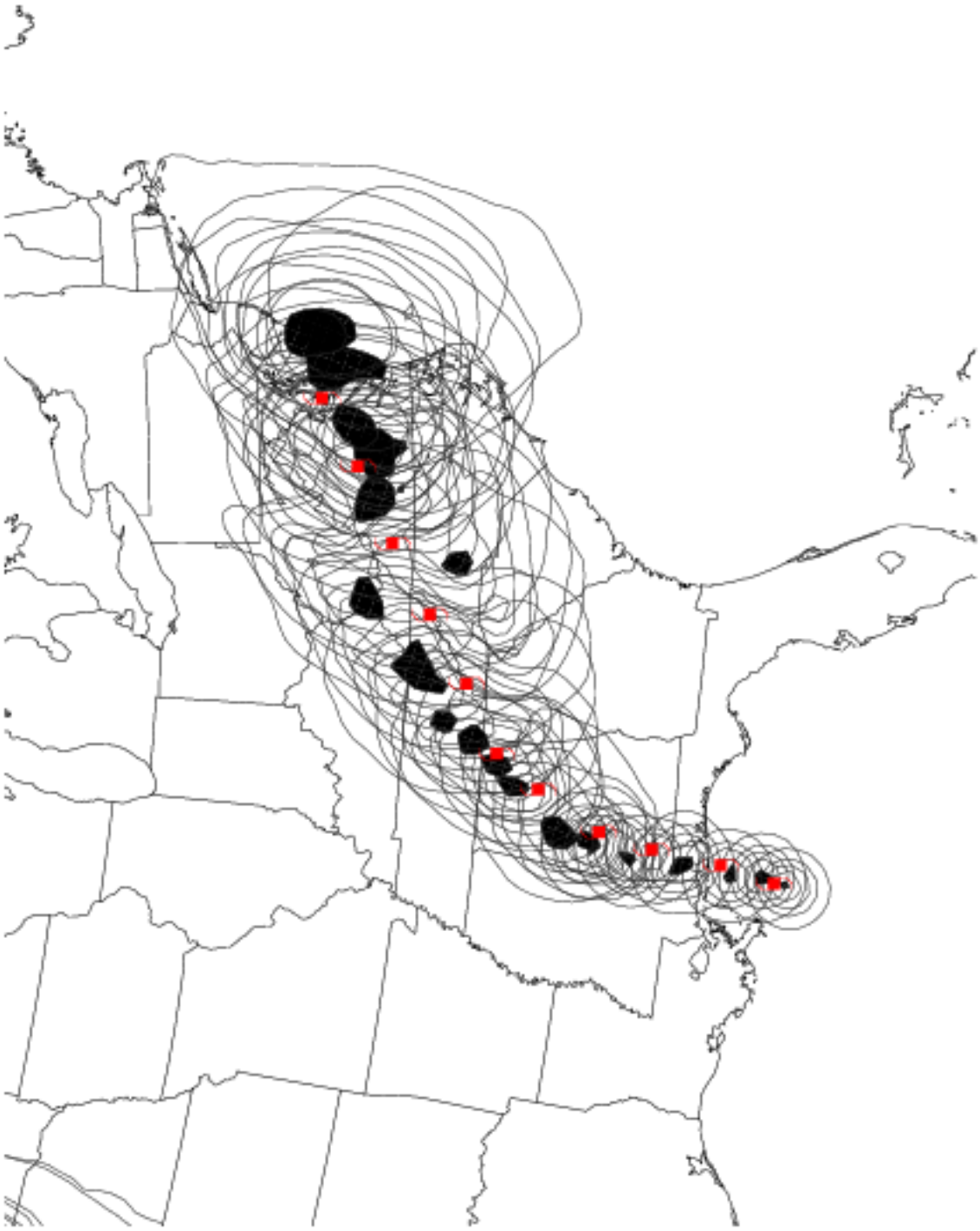

Figure 4: Ivan track given by pressure perturbations of 0.25, 1, 2, 3, and 5hPa above minimum - NARR reanalysis vs observed (red symbols)

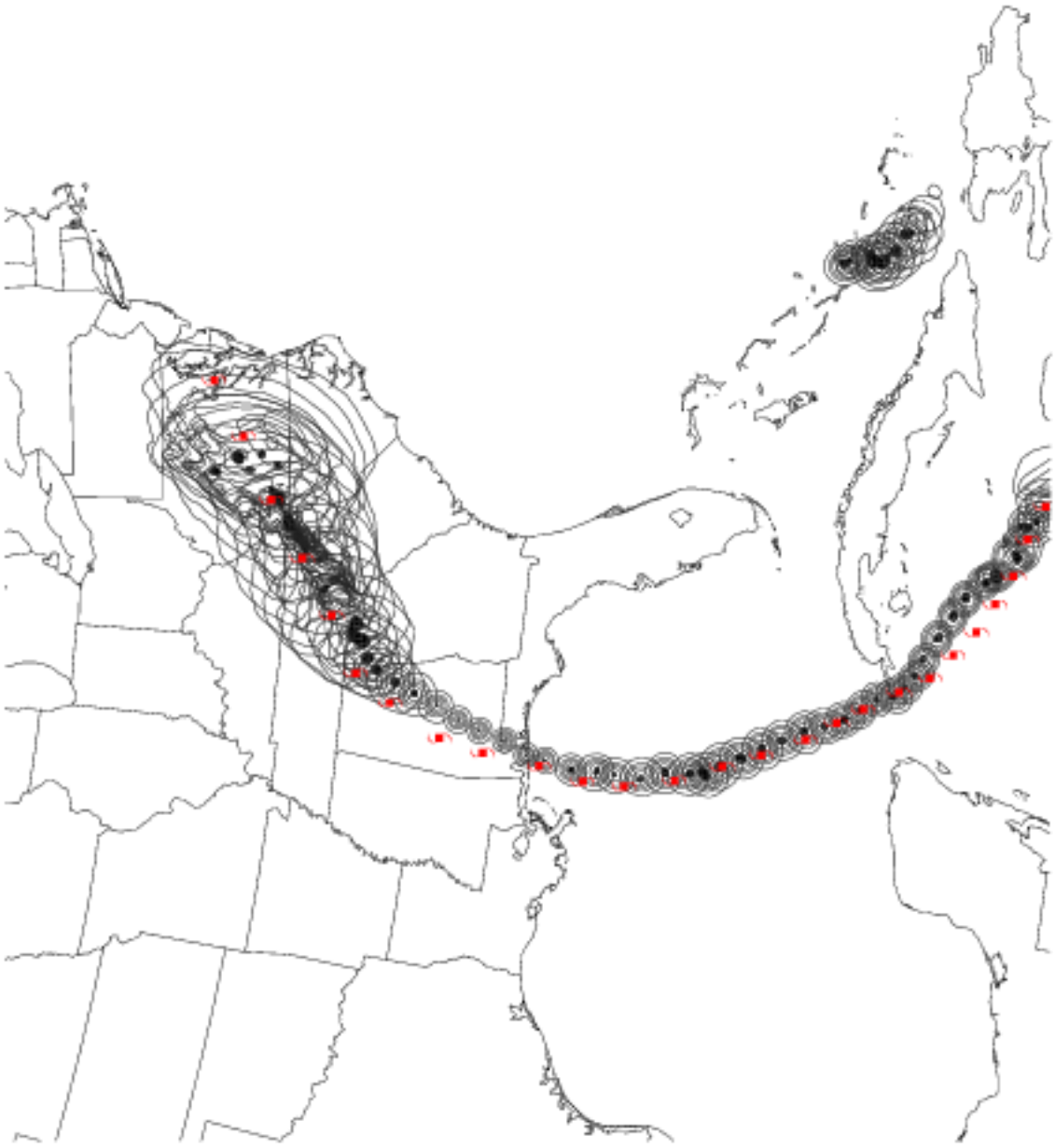

Figure 5: As in figure 4, but for the TOPO simulation

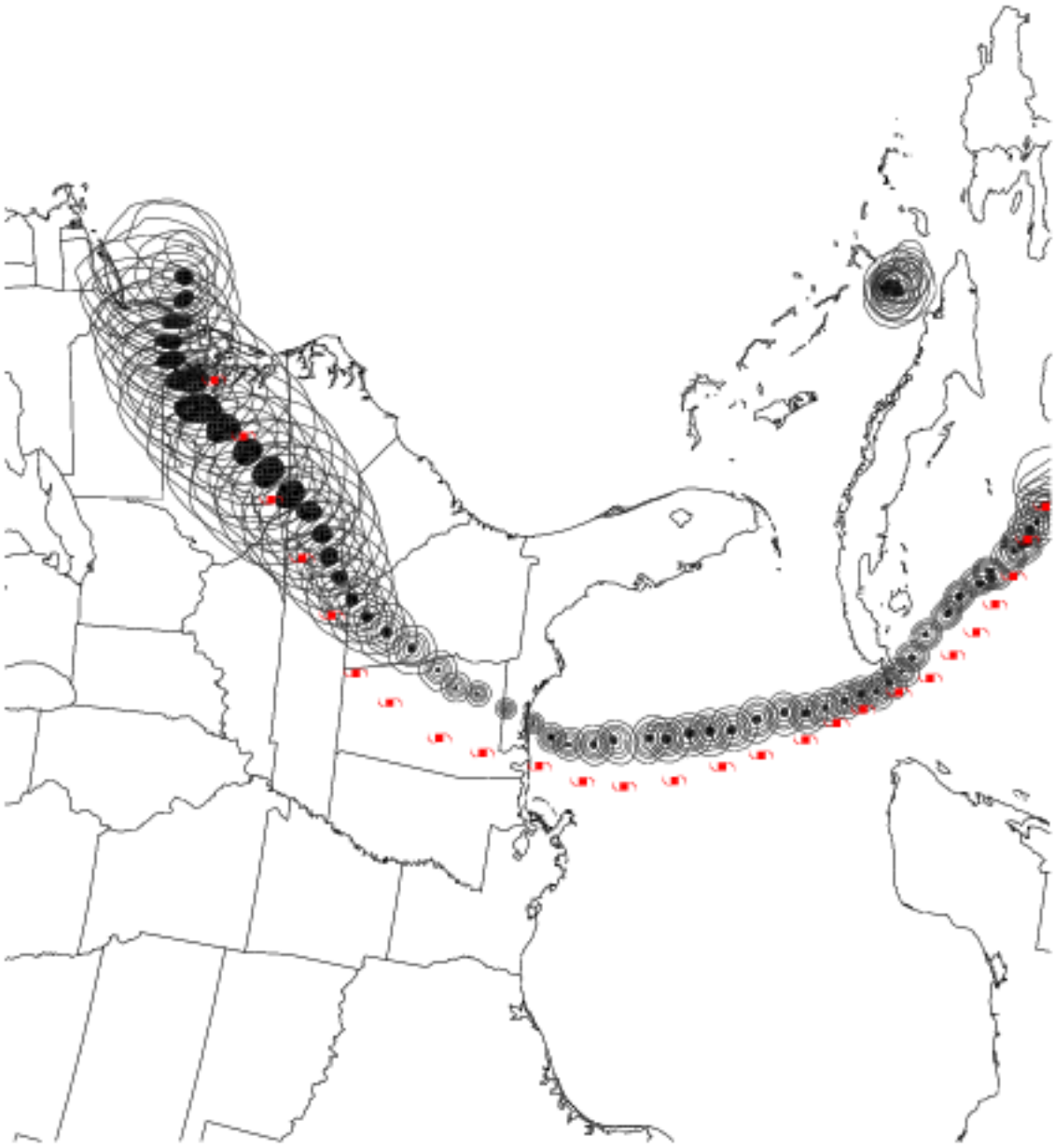

Figure 6: As in figure 4, but for the UNTOPO simulation

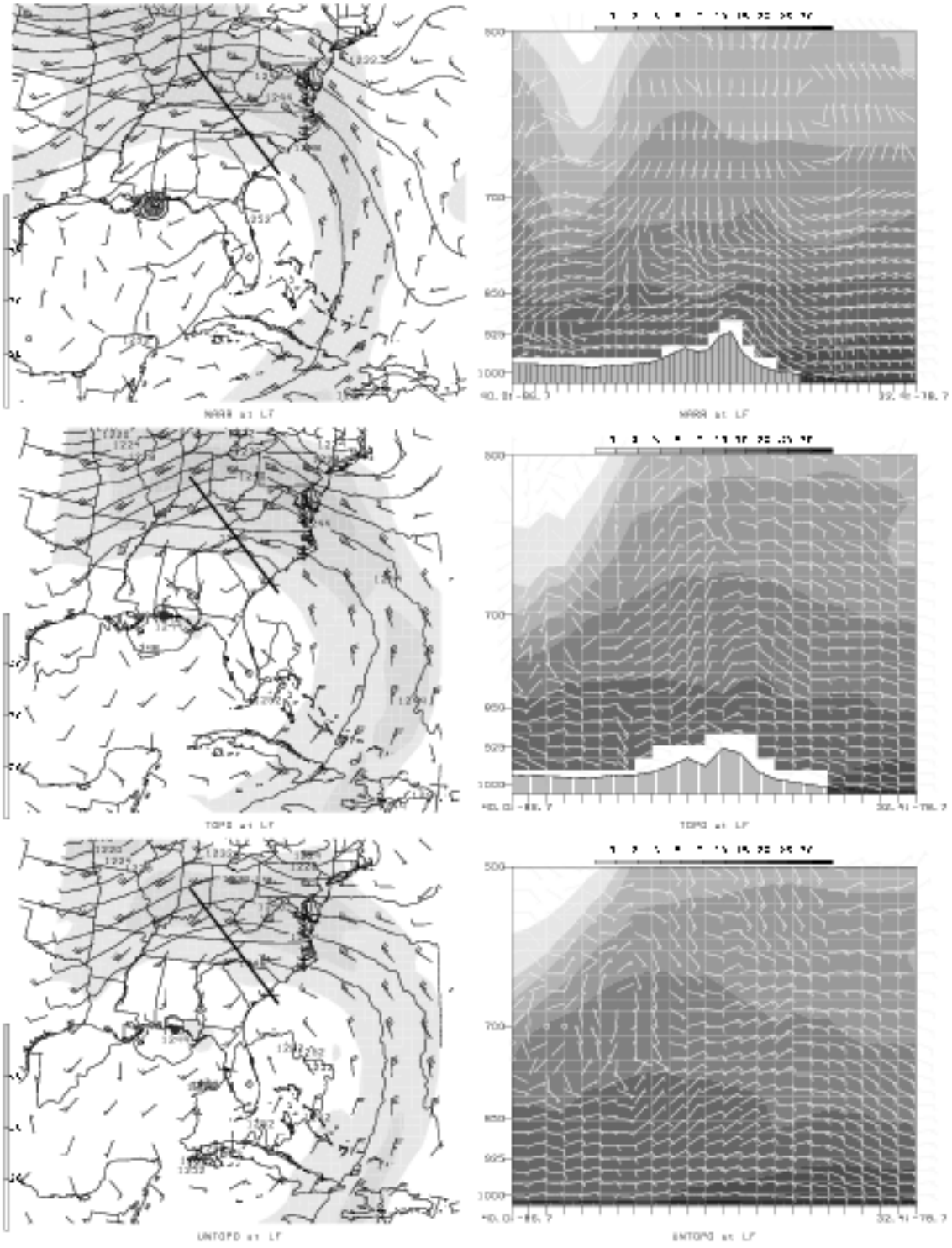

Figure 7: 200hPa geopotential heights (dam) and winds (ms^{-1}) (left), and cross sections of moisture (g/kg) during Ivan: NARR (top), TOPO run (center), UNTOPO run (bottom)

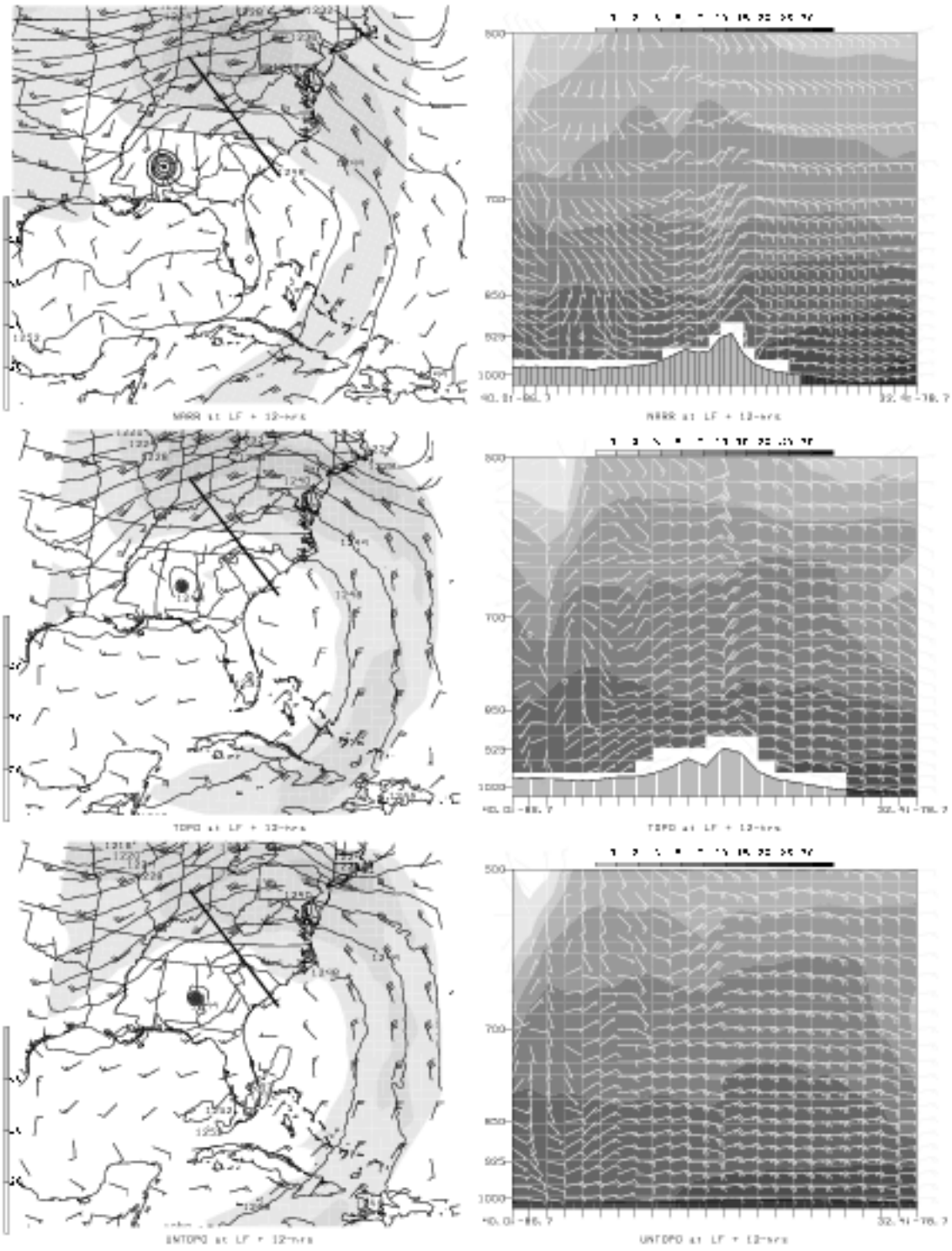

Figure 8: As in Fig. 7 at post-landfall times indicated above: NARR (top), TOPO run (center), UNTOPO run (bottom)

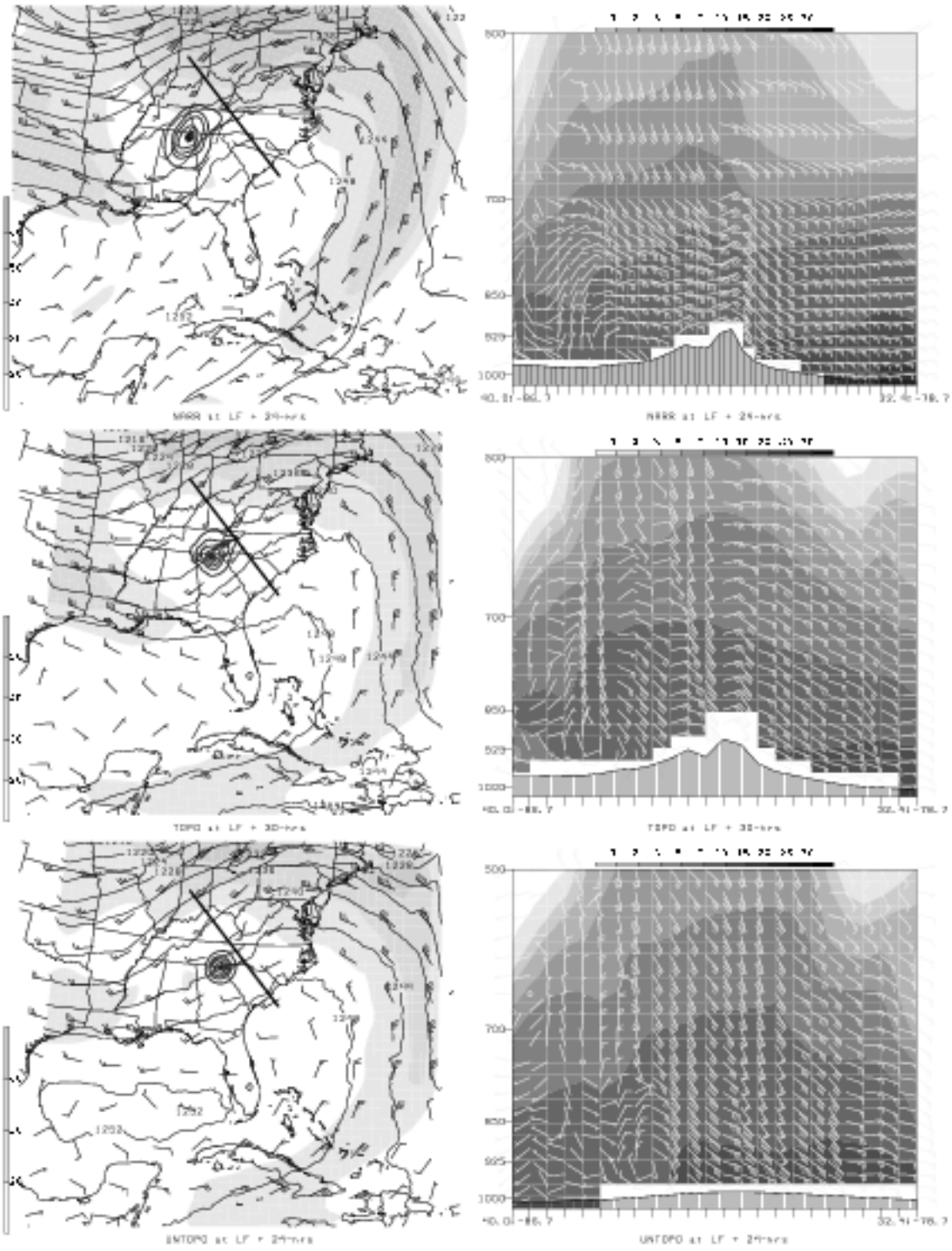

Figure 9: As in Fig. 7 at post-landfall times indicated above: NARR (top), TOPO run (center), UNTOPO run (bottom)

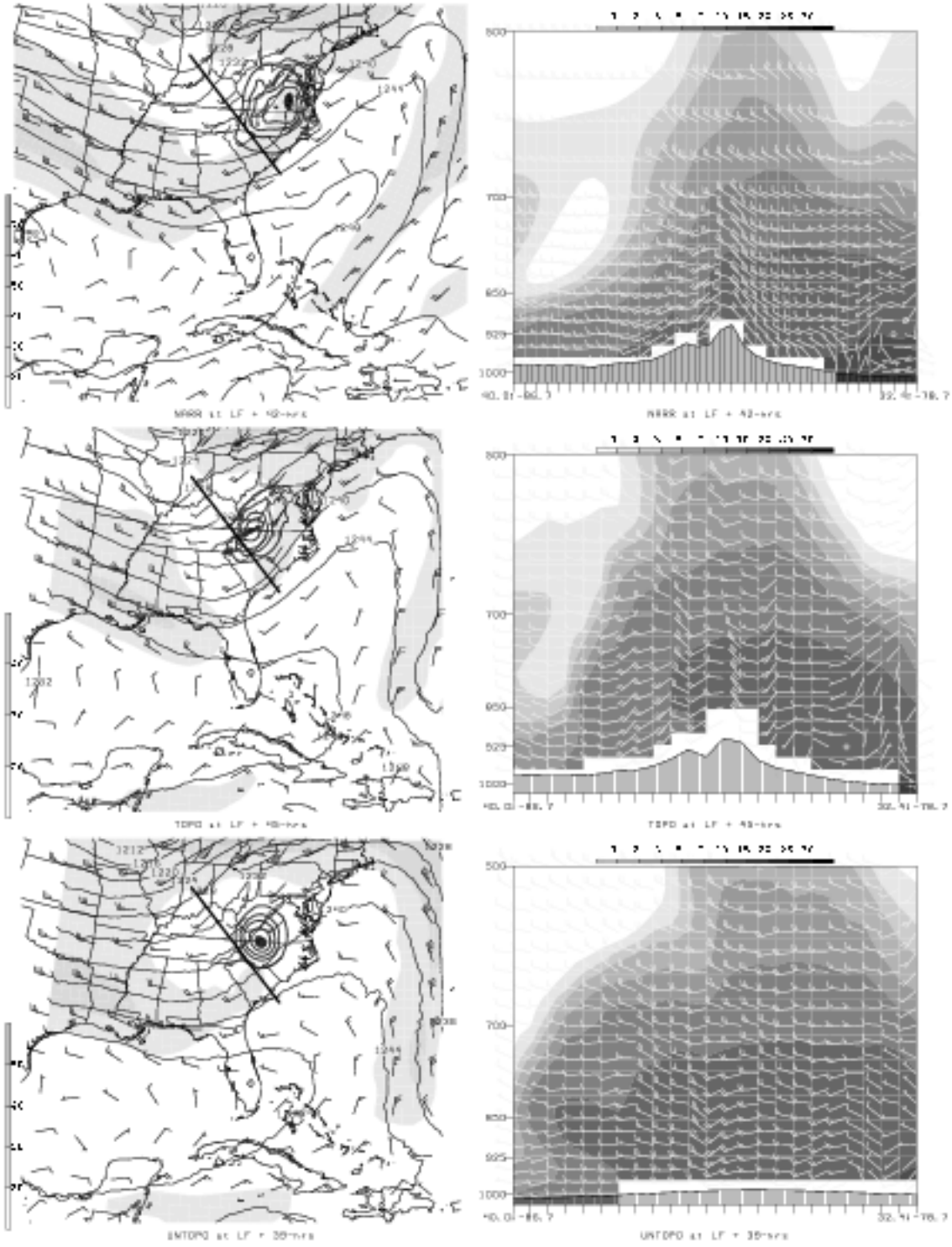

Figure 10: As in Fig. 7 at post-landfall times indicated above: NARR (top), TOPO run (center), UNTOPO run (bottom)

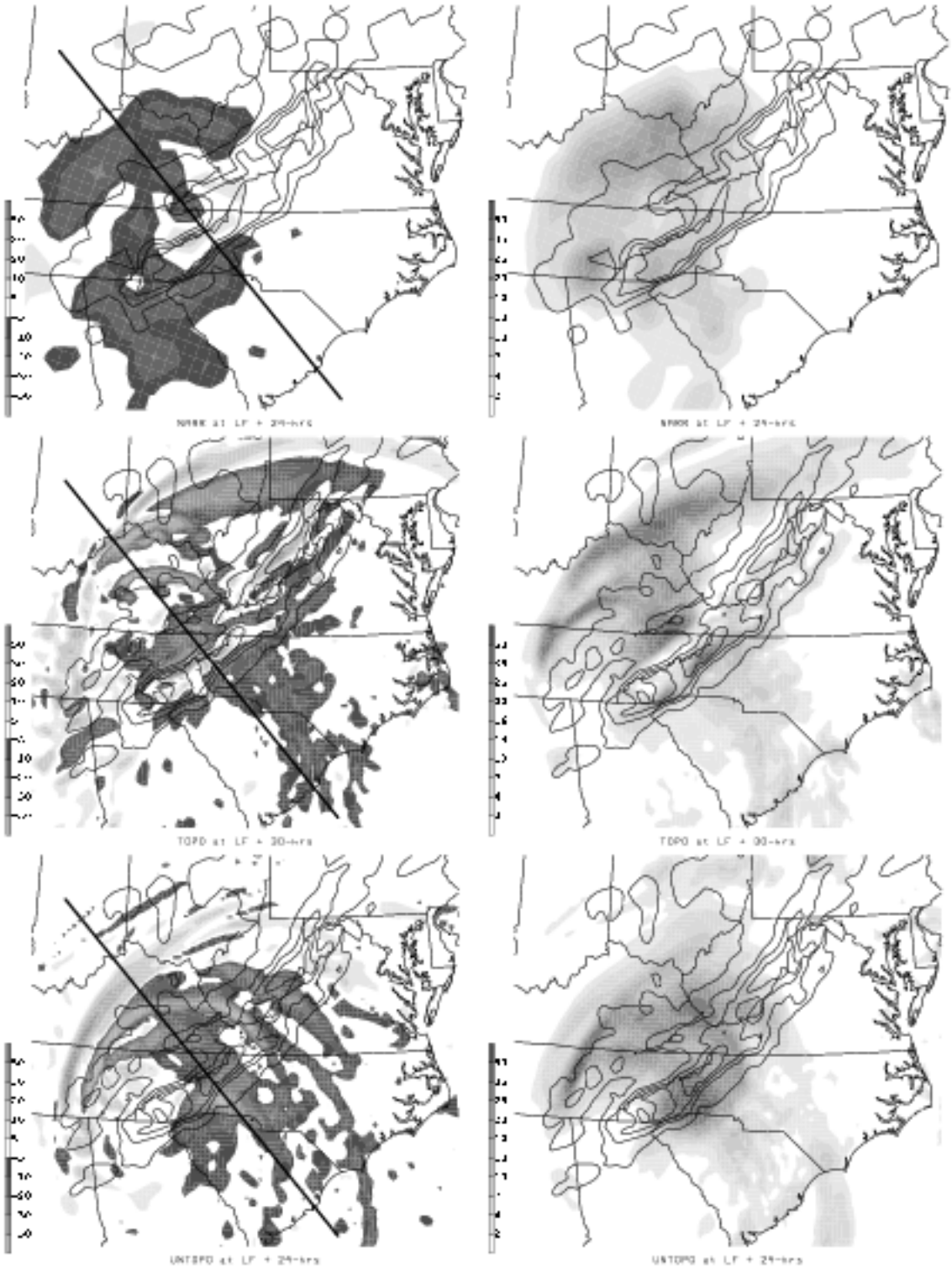

Figure 11: Hurricane Ivan ω (in μbs^{-1} on left) and 3-hour precipitation (in mm on right) occuring with figure 9: NARR (top), TOPO run (center), UNTOPO run (bottom)

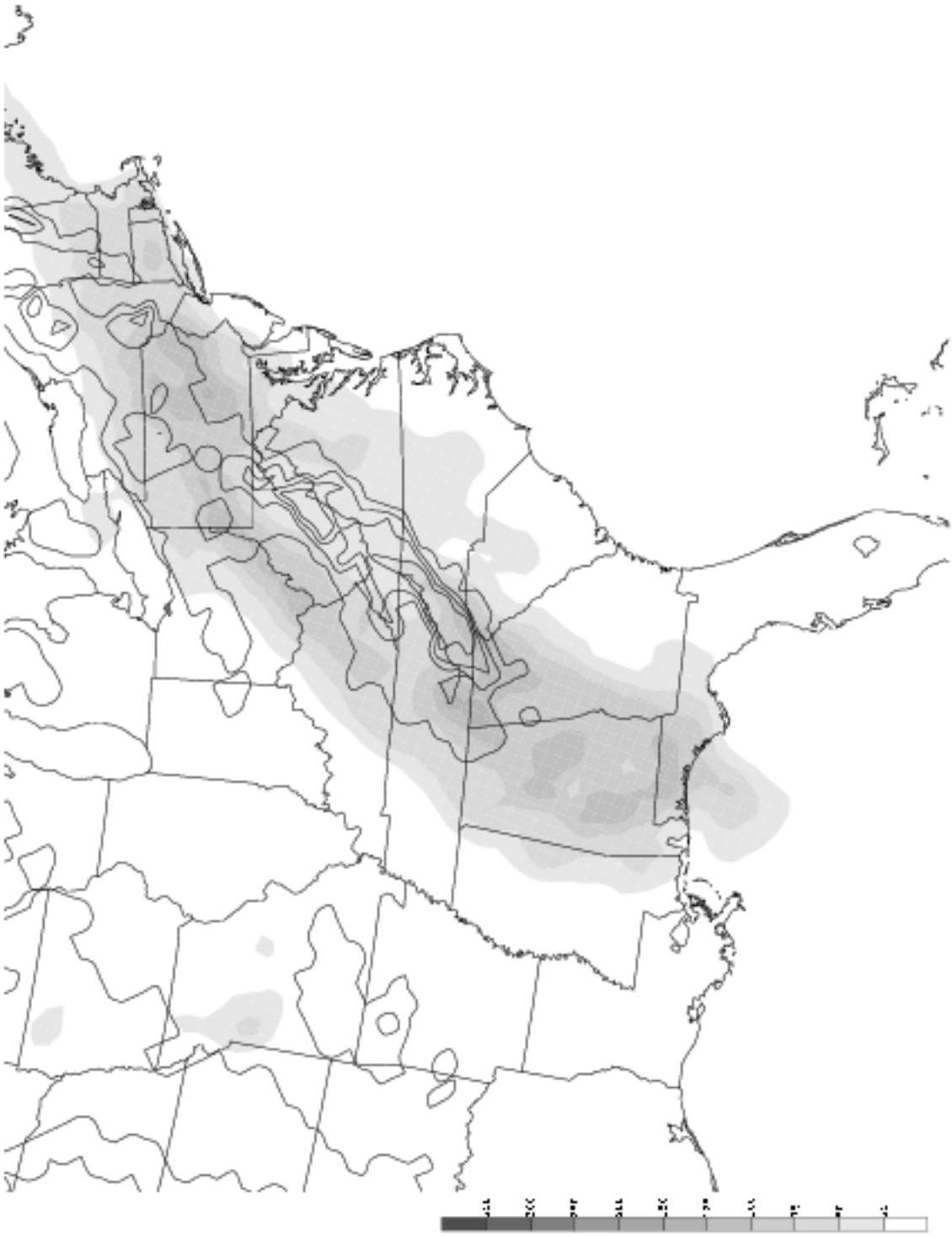

Figure 12: Total precipitation (mm) - NARR reanalysis

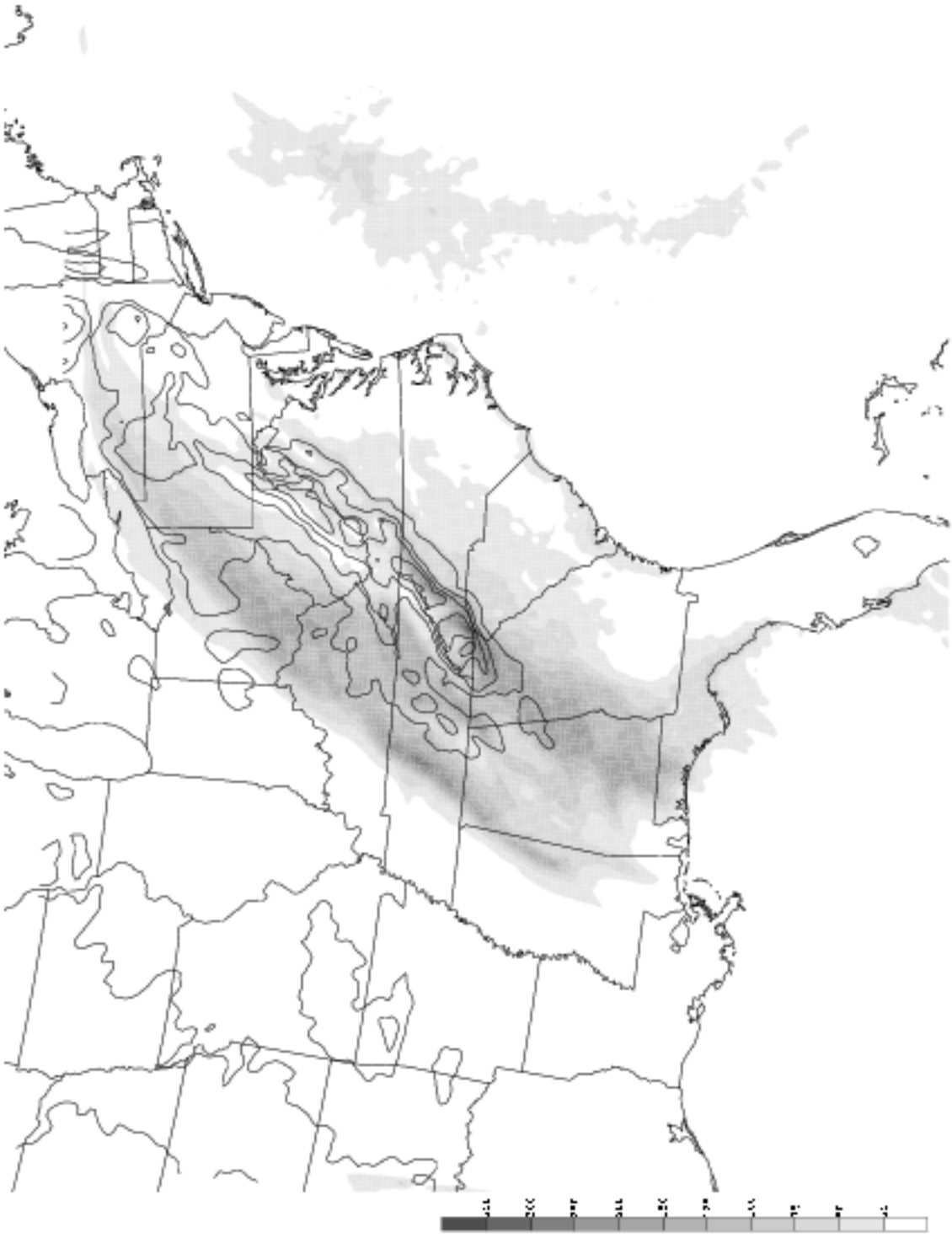

Figure 13: Total simulated precipitation (mm) - TOPO model run

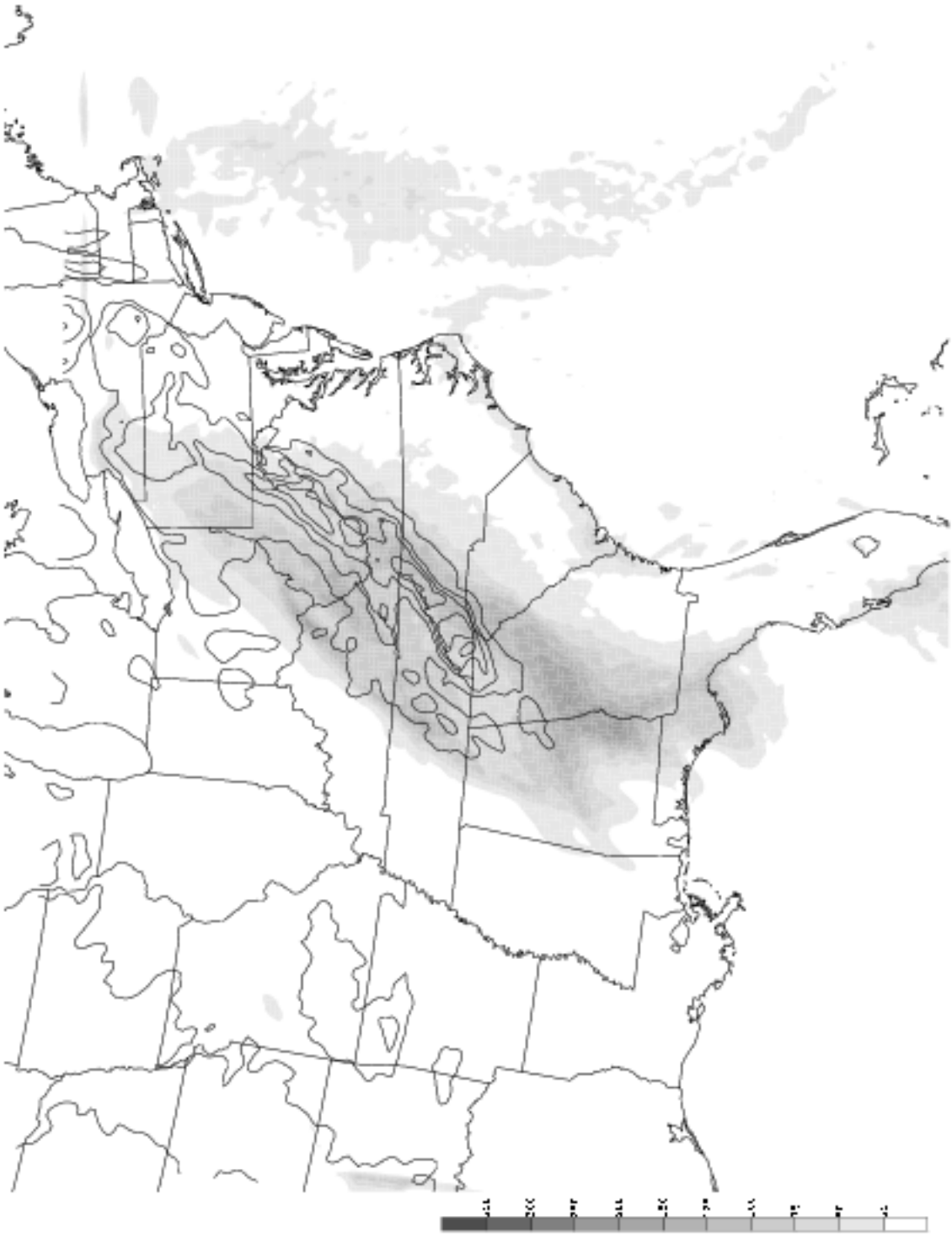

Figure 14: Total simulated precipitation (mm) - UNTOPO model run

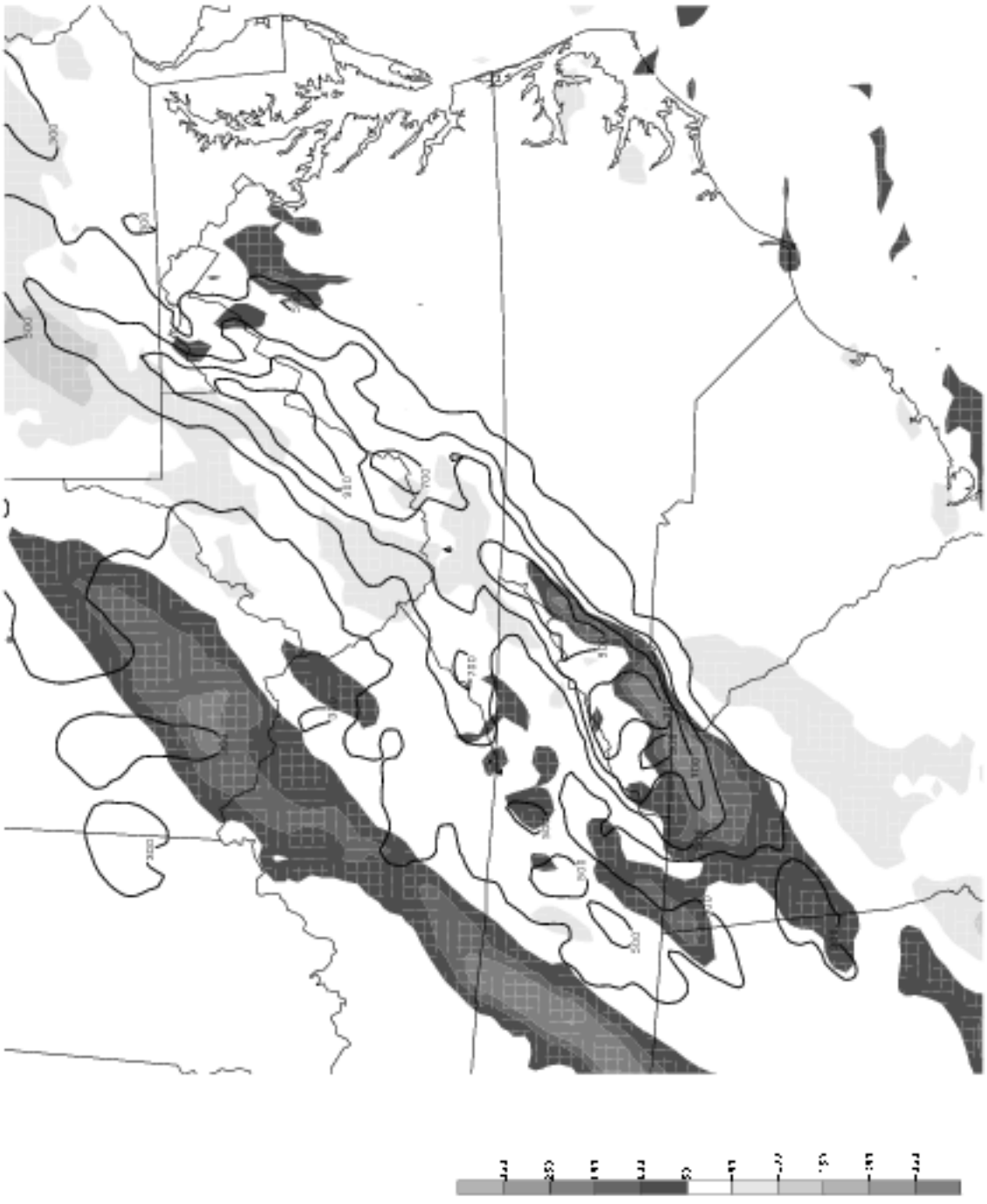

Figure 15: Ivan total simulated precipitation (mm) difference: TOPO - UNTOPO